Dependence on initial conditions in nonlocal PDE's and hereditary dynamical systems

Rebecca Crabb, Jérôme Losson and Michael C. Mackey

Abstract. Solution sensitivity to initial conditions in a first order delayed partial differential equation is investigated around the Hopf bifurcation and around higher order bifurcations. The presence of multistable limit cycles and the geometry of their basins of attraction are then investigated systematically for three different first order nonlinear ordinary differential delay equations.

1991 Mathematics Subject Classification: 34A34, 35B30, 35B40.

1. Introduction

In this paper, we investigate the dependence of solution behavior on perturbations of the initial conditions in a class of delayed differential equations. The first system considered is a model for proliferating and maturing cell populations framed as a first nonlinear delayed partial differential equation (DPDE). Solution dependence on initial conditions if first discussed around the Hopf bifurcation (Section 3) and then around higher order bifurcations (Section 4).

One technique used to study solution dependence on initial conditions is the method of characteristics. Along the characteristics, the DPDE reduces to an ordinary differential delay equation (ODDE). This led us to investigate solution dependence on perturbations of the initial functions in different ODDE's in Section 5.

2. A model for proliferating and maturing cellular populations

We consider a model for cell replication in which the cells are both proliferating and maturing [9, 10].

Let a denote the cell age, x the maturation variable, t time, γ the rate at which cells die, and $V(x)$ the maturation velocity where a ranges from 0 to τ and x

ranges from 0 to 1. If $U(t,x,a)$ denotes the density of proliferating cells then

$$\frac{\partial U}{\partial t}+\frac{\partial U}{\partial a}+\frac{\partial[V(x)U]}{\partial x}=-\gamma U \tag{1}$$

is the conservation equation for $U(t,x,a)$ with initial condition

$$U(0,x,a)=\Gamma(x,a) \text{ for } (x,a)\in[0,1]\times[0,\tau].$$

The total number of proliferating cells is given by

$$u(t,x)=\int_0^\tau U(t,x,a)da$$

and the boundary conditions for the system are

$$U(t,x,0)=2U(t,x,\tau)=\mathcal{F}(u(t,x))$$

where $\mathcal{F}$ is the input flux of the total number of cells at a given maturation level.

If we assume that the maturation velocity V is given by

$$V(x)=rx,\ r>0,$$

then integrating (1) over the age variable a and applying the boundary conditions, yields

$$\frac{\partial u}{\partial t}+rx\frac{\partial u}{\partial x}=-\delta u+\lambda u_\tau(1-u_\tau) \tag{2}$$

where the input flux $\mathcal{F}$ has been taken as

$$\mathcal{F}(u)=u(1-u),$$

and δ,λ and u_τ are defined by

$$\delta=\gamma+r,\ \lambda=ce^{-(\gamma+r)\tau},\ u_\tau\equiv u(t-\tau,xe^{-r\tau}).$$

The initial condition is:

$$u(t-\tau,xe^{-r\tau})=\varphi(x) \text{ for } (t,x)\in[0,\tau]\times[0,1]. \tag{3}$$

We pick $\tau=1$ without loss of generality.

3. Solution behavior around the Hopf bifurcation

In this section, we summarize some of the results from Rey and Mackey [9, 10]. We consider the effects of two slightly different initial functions $\varphi(x)=x+0.1$ and $\varphi(x)=x$. To study the effects of these initial functions two numerical approaches are used: the Galerkin finite elements method and the method of characteristics.

When $\varphi(x)=x+0.1$, for $0<\lambda<\delta$ the trivial solution is the only biologically meaningful stationary spatially homogeneous solution. For $\lambda>\delta$ there is a second stationary spatial solution, $(\lambda-\delta)/\lambda$, which coexists with the trivial solution. When (2) is linearized about either steady state, it yields a single bifurcation diagram

consisting of three regions: two stationary spatially homogeneous solutions and a periodic spatially homogeneous solution delimited by the line $\lambda = \delta$ and by the Hopf bifurcation curve.

When $\varphi(x) = x$, for $0 < \lambda < \delta$ the trivial solution is again the single stationary solution. For $\lambda > \delta$ there is no longer a unique globally asymptotic stable steady state, instead there are three families of stationary solutions: a trivial solution, a spatially nonhomogeneous solution $\lambda = (\delta + r)e^{rt}$,

$$\text{and a singular solution} \begin{cases} 0 & \text{when } x = 0 \\ \frac{\lambda - \delta}{\lambda} & \text{when } x > 0 \end{cases}$$

depending on the values of (δ, λ, r). By linearizing (2), we obtain three bifurcation diagrams depending on whether r is less than, greater than, or equal to 1. For $r = 0.7455$, the bifurcation diagram consists in three regions: two stable stationary solutions and a traveling wave solution delimited by the stationary nonhomogeneous solution and the Hopf bifurcation. For $r = 1$, the bifurcation diagram consists in three regions: two stable stationary solutions and a slow traveling wave solution again delimited by the stationary nonhomogeneous solution and the Hopf bifurcation. For $r = 1.1$, the bifurcation diagram consists in only two regions: a stable stationary solution and a chaotic waves solution delimited by the stationary nonhomogeneous solution.

4. Higher order bifurcations

In Figure 1, λ is plotted versus the period of $u(t)$ while δ and r remain fixed. Figure 1 shows that the Hopf bifurcation occurs at $\lambda \simeq 4.3$ followed by a higher order bifurcation at $\lambda \simeq 5.3$. At $\lambda \simeq 5.8$ the numerical solution appears to be "turbulent". This is followed by a reverse bifurcation as λ increases further. One can see this in Figure 2 where the local extrema of $u(t)$ are plotted as a function of λ.

Focusing on the area between $\lambda = 5.7$ and $\lambda = 5.9$, Figure 3 clarifies the transition from the higher order bifurcations to the turbulent solution behavior and from the turbulent solution behavior to the reverse bifurcation.

The initial function used to obtain Figures 1-3 was $\varphi(x) = x$. To obtain these figures, we used the method of characteristics: (2) is rewritten as

$$\frac{du}{dt} = -\delta u + \lambda u_\tau (1 - u_\tau) \tag{4}$$

along the x characteristic, $x(t) = \epsilon e^{rt}$, where

$$u(t, x(t)) \equiv u(t, x(t) = \epsilon e^{rt})$$

and

$$u_\tau(t, x(t)) \equiv u\left(t - 1, \epsilon e^{r(t-1)}\right).$$

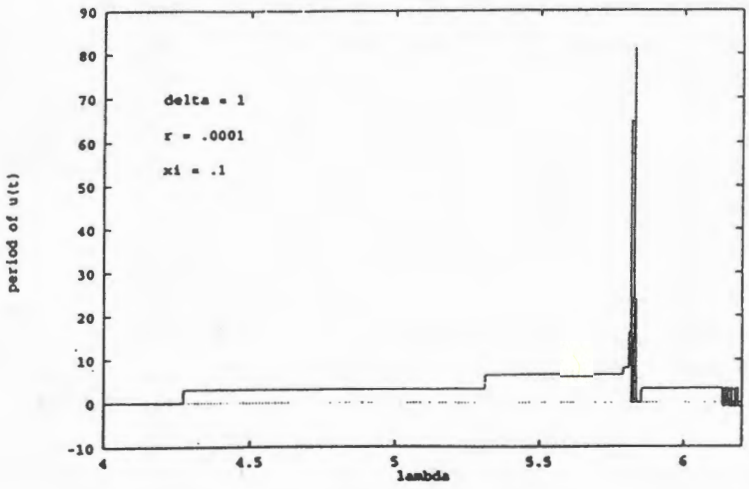

Figure 1. Higher order bifurcations $\delta = 1$, $r = .001$. When the period equals 0 the solution is chaotic, when the period equals -1 the solution diverges to $-\infty$.

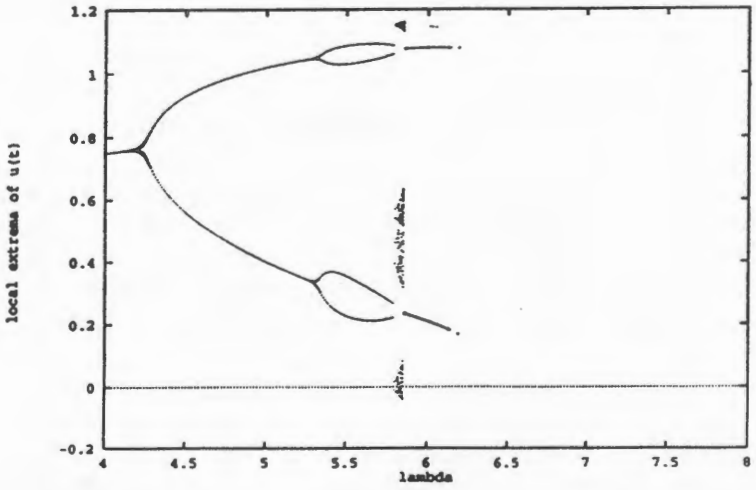

Figure 2. Local extrema of $u(t)$ versus λ for the same δ and r as in Figure 1. Here we can clearly see the Hopf bifurcation, the chaotic windows, and the reverse bifurcation.

We now take as an initial condition the time segment $[,0,,\tau]$ of the solution of (4) for $\lambda = 5.7$ which was generated by $\varphi(x) = \epsilon e^{rt}$ for $t \in [-\tau, 0]$. r, δ, and ϵ are the same as in Figure 3. The turbulence has completely disappeared and instead there is a smooth transition from the first bifurcation to the reverse bifurcation. Other interesting behavior has been observed by using the solutions of (4) for various λ's as initial function.

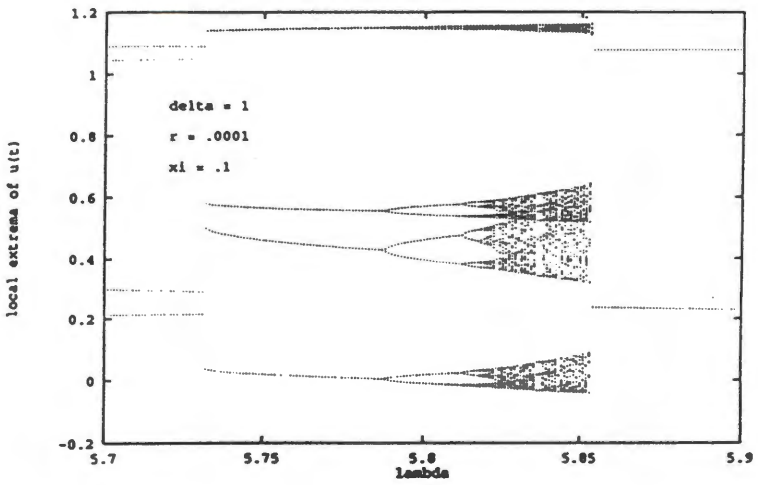

Figure 3. Blow up of the local extrema of $u(t)$ versus λ for $\delta = 1$ and $r = .0001$ for $\lambda \in [5.7, 5.9]$ where the initial condition is $u(t-1, xe^{-r}) = x = \varphi(x)$.

The only difference between Figures 3 and 4 is a change in the initial function. This clearly indicates that the asymptotic behavior of the solutions of (4) is sensitive to changes in the initial function. In the next section, we investigate this property in (4) as well as in two closely related equations.

5. Multistability in first order ODDE's

We consider in this section the dynamics of first order differential delay equations. The equations describe the evolution of a variable x which is being destroyed at a rate δ and produced, with some delay, *via* a nonlinear production mechanism:

$$\frac{dx}{dt} = -\delta x + F(x_\tau), \quad \delta, \tau \in \mathbb{R}^+, \tag{5}$$

where $x_\tau \equiv x(t-\tau)$. F, the *feedback function*, is the rate of production which depends on the history of the variable. The initial function is denoted by φ:

$$x(t) \equiv \varphi(t) \text{ for } t \in [-\tau, 0).$$

The wealth of dynamics displayed by equation (5) depends to a great extent on the feedback F. We are interested here in the case where F is nonmonotone, modeling so-called *mixed feedback* control loops. Although (5) looks simple, it corresponds to a class of semidynamical systems which can display a remarkable range of solutions: from steady states bifurcating to limit cycles of arbitrary complexity to chaotic trajectories as a control parameter is varied [2, 6].

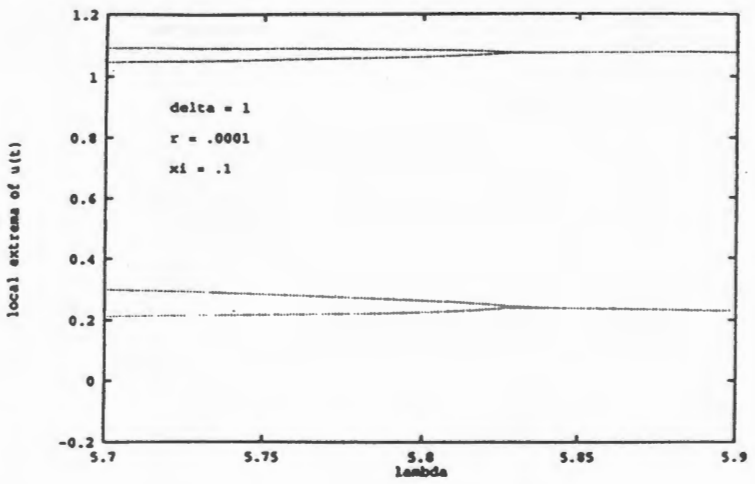

Figure 4. Local extrema of $u(t)$ versus λ for $\delta = 1$ and $r = .0001$ where the initial condition is $u(t-1, xe^{-r}) =$ solution for $\lambda = 5.7$.

Equations like (5) have been used to describe the dynamics of physiological control systems [8], multistable optical devices [1, 3, 4, 5] (and references therein), and agricultural commodity markets [7], to mention a few applications. They also provide a natural extension of one dimensional discrete-time maps. This extension makes use of a simple singular perturbation limit procedure: In (5), taking the limit $\delta \to \infty$, keeping F/δ finite, and then discretizing time in units of τ yields a 1-d map [6].

We study the problem of solution multistability in these differential equations by focusing on three paradigm systems.

5.1. The logistic ODDE

The logistic ODDE,

$$\frac{dx}{dt} = -\delta x + \lambda x_\tau (1 - x_\tau), \ \ \lambda \in \mathbb{R}^+ \tag{6}$$

is constructed as the singular perturbation of the logistic map. We encountered this equation in the first part of this paper since it is the x characteristic of equation (2).

The initial functions we consider are

$$\varphi(t) = A \sin(\omega t) + B, \ \ A, \omega \in \mathbb{R}^+, \ \ B \in \mathbb{R}.$$

Figure 5 displays bistable limit cycle solutions of (6).

It appears numerically that the bistable limit cycles are born out of a single limit cycle which loses stability as two stable ones arise. The single original limit

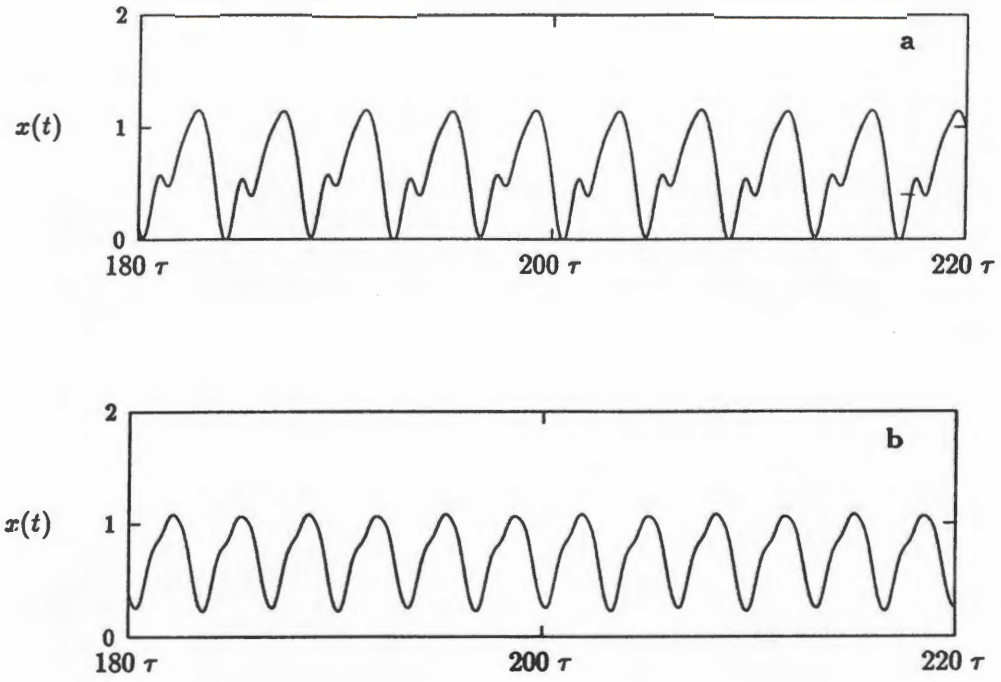

Figure 5. Two coexisting solutions of (6). The parameter values in both cases are $\delta = 1$, $\lambda = 5.81$, $\tau = 1$. **a)** The initial function is $\varphi(t) = 0.4 \sin(0.3t) + 0.5$. **b)** The initial function is now $\varphi(t) = 0.4 \sin(1.3t) + 0.5$.

cycle is a descendant of the Hopf cycle around the unstable positive fixed point. Figure 6 shows the structure of the basins of attraction of the two cycles displayed in Figure 5.

This sensitive dependence on the initial conditions is common in nonlinear dynamical systems, but it has not been described for delay systems in the past. We now show that a different kind of bistability is observed in a similar system which has also been used as a model in biomathematics.

5.2. The Mackey-Glass equation

The following equation was first introduced as an attempt to model the oscillations of neutrophils observed in some cases of chronic myelogenous leukemia [8]:

$$\frac{dx}{dt} = -\delta x + \frac{\beta x_\tau}{1 + x_\tau^n}. \tag{7}$$

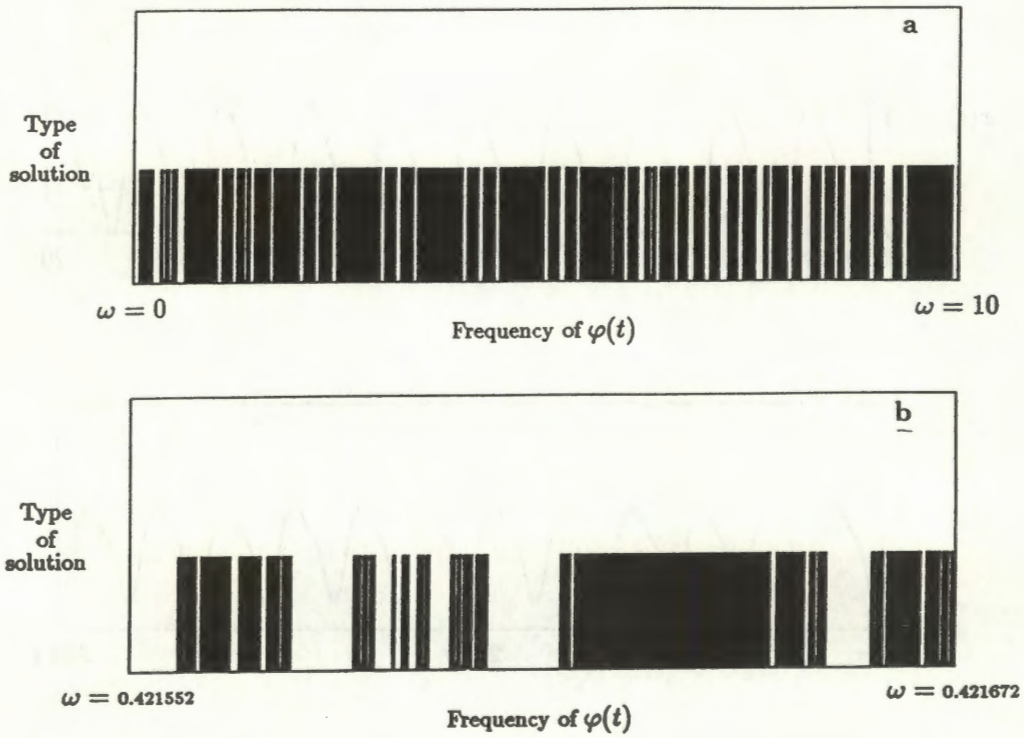

Figure 6. This figure displays which values of ω (the frequency of φ) give rise to the solution of Figure 5b, keeping all other parameters at the values specified in Figure 5b. The vertical bars are placed at the values of ω giving rise to the solution of Figure 5b. The part **(a)** the ODDE (6) was solved with 5000 different values of ω uniformly distributed between 0 and 10. In part **(b)** (6) was solved with 500 different values of ω distributed uniformly between 0.421552 and 0.421672. No other solution types were observed for these parameter values. The convergence time t_c to the asymptotic limit cycle ranges from $t_c \simeq 10$ delays to $t_c \simeq 6000$ delays, depending on ω in a complex manner.

Equation (7) possesses steady, periodic, and aperiodic solutions in different regions of parameters space (*ibid.*).

If n is even, (7) is invariant under the transformation $x(t) \to -x(t)$. This bistability is illustrated in Figure 7. It appears numerically that the bistable limit cycles arise from the two Hopf cycles around the nonzero fixed points. No stable limit cycle around the origin was found.

The bistability in the Mackey-Glass equation may be a simple example of a more general situation: an equation possessing invariance under a coordinate transformation will display bistability between one limit cycle and its transformed version.

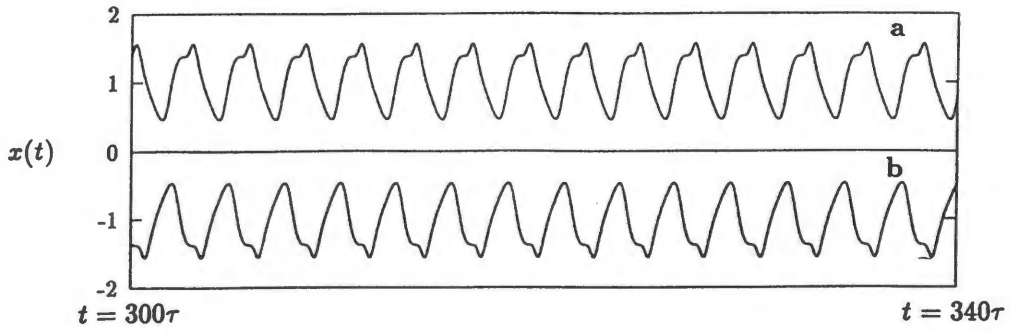

Figure 7. Two bistable solutions of the Mackey-Glass equation. The parameters in both panels are $\delta = 1$, $\beta = 3$, $n = 8$, $\tau = 1.25$. The initial function in both is $\varphi(t) = 1.5\sin(\omega t) + 0.6$. In **a)** $\omega = 0.3$. In **b)** $\omega = 0.7$. Transients were discarded.

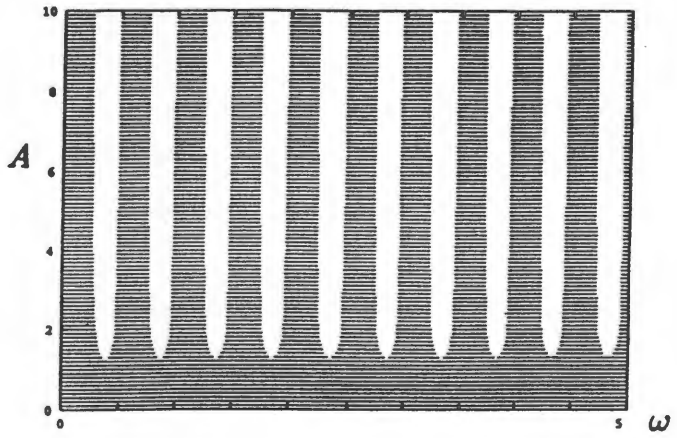

Figure 8. This figure displays a subset of the basin of attraction for the solution of (7). Every black dot represents a locus in $A - \omega$ space giving rise to the limit cycle shown in Figure 7a. The initial functions were $\varphi = A\sin(\omega t) + 1$. The white areas do not dip below 1 since a strictly positive (negative) φ gives rise to a strictly positive (negative) solution.

The apparent simplicity of Figure 8 could make the Mackey-Glass equation an interesting candidate for an analytic investigation of the structure of its basins of attraction. Such a discussion falls outside the scope of this paper, and we now examine the cubic ODDE which displays a bistability due to its invariance under $x(t) \to -x(t)$ and bistability between strictly positive (negative) limit cycles reminiscent of the behavior displayed by the logistic ODDE.

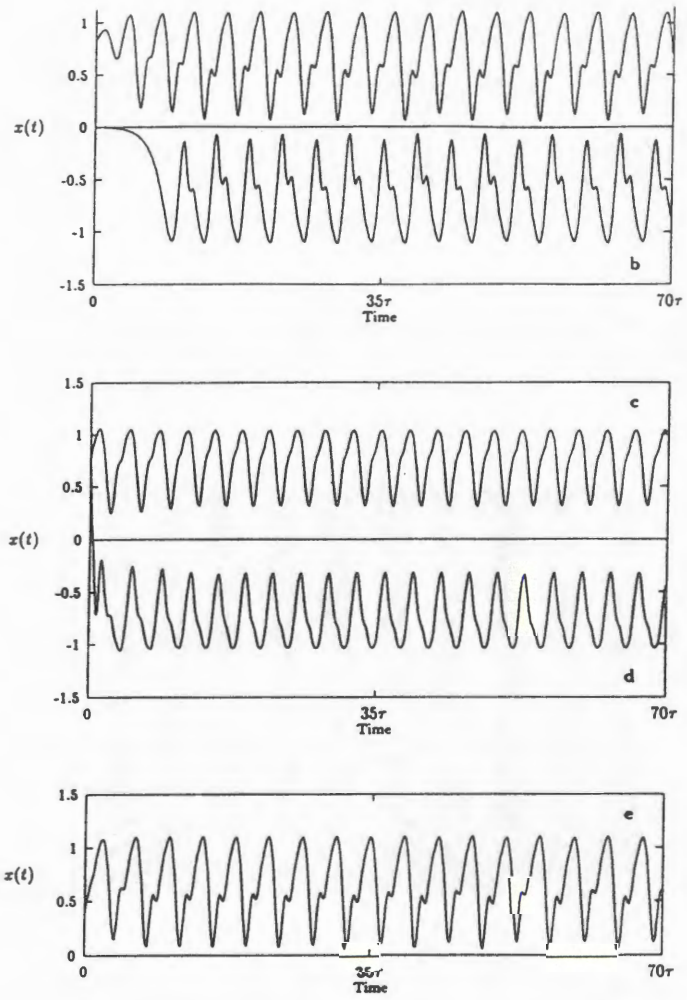

Figure 9. Several multistable solutions of equation (8). In all five panels, the parameters are $\delta = 1$, $\lambda = 3.5$, $\tau = 1$. The quantity which is being varied in the figure is the offset B of the initial function. In **a** $\varphi = 0.01\ \sin(3.6t) + 1.3$. In **b** $\varphi = 0.01\ \sin(3.6t)$. In **c** $\varphi = 0.01\ \sin(3.6t) + 1.1$. In **d** $\varphi = 0.01\ \sin(3.6t) + 1.2$. In **e** $\varphi = 0.01\ \sin(3.6t) + 0.3$.

5.3. The cubic ODDE

The cubic ODDE is equation (5) with a cubic odd nonlinearity:

$$\frac{dx}{dt} = -\delta x + \lambda x_\tau (1 - x_\tau^2), \quad \delta, \lambda \in \mathbb{R}^+. \tag{8}$$

We study the multistability in (8) with sinusoidal initial functions, and illustrate numerically that it displays a bistability due to its invariance under the transformation $x(t) \to -x(t)$, and bistability reminiscent of the situation discussed in Section 5.1: Thus, two positive cycles arise from a single positive limit cycle which loses its stability at a bifurcation point.

Preliminary numerical results indicate that the structure of subsets of the basins of attraction will be as complicated in this equation as they were in the logistic ODDE. Numerical simulations of ODDE's is computationally costly. It is therefore desirable to introduce a nonlinear first order ODDE which is known to display the wealth of dynamics characteristic of nonlinear first order ODDE's while remaining tractable analytically.

6. Conclusion

The first order delayed partial differential equation (2) shows sensitivity to small perturbations to the initial function, φ, around the Hopf bifurcation. For $\varphi(x) = x + 0.1$, just past the Hopf bifurcation, the solution is periodic spatially homogeneous. For $\varphi(x) = x$, just past the Hopf bifurcation, the solution consists in either traveling waves or chaotic waves depending on (λ, δ, r). This DPDE also shows sensitivity to the initial condition around higher order bifurcations.

Asymptotic solution behavior in first order ODDE's can depend in a sensitive way on the initial function. In some cases, the basins of attraction of multistable limit cycles appear to possess intricate structure at all scales. One possible mechanism giving rise to bistability in ODDE's, is invariance of the ODDE under a coordinate transformation. A simple example of this mechanism is observed in the Mackey-Glass equation. In the logistic ODDE and the cubic ODDE the origin of multistable cycles can be described as follows: A single stable limit cycle loses its stability at a bifurcation point, and two new stable limit cycles appear. These bifurcations giving rise to multistability are observed far from the Hopf bifurcation(s) at the fixed point(s).

References

[1] Gibbs, H.M., Hopf, F.A., Kaplan, D.L. and Shoemaker, R.L., Observation of chaos in optical bistability, Phys. Rev. Lett. 46 (1981), 474

[2] an der Heiden, U., In: Delay equations: Approximation and application (ed. by G. Meinardus and G. Nunburger), Intern. Ser. Num. Math 74 (1985), Birkhäuser, Basel

[3] Hopf, F.A., Meystre, P., Drummond, P.D. and Walls, D.F., Anomalous switching in dispersive optical bistability, Optics. Comms. 31 (1982), 245
[4] Ikeda, K., Multiple-valued stationary state and instability of the transmitted light by a ring cavity system, Opt. Commun. 30 (1979), 257
[5] Ikeda, K. and Akimoto, O., Successive bifurcations and dynamical multistability in a bistable optical system: A detail study of the transition to chaos, Appl. Phys. 28b (1979), 170
[6] Ivanov, A.F. and Sharkovskiĭ, A.N., Oscillations in singularly perturbed delay equations, Dynamics Reported (ed. by H.O. Walter and U. Kirchgraber) 3(1991), 165, Springer-Verlag
[7] Mackey, M.C., Commodity price fluctuations: Price dependent delays and nonlinearities as explanatory factors, J. Econ. Theory 48 (1989), 497
[8] Mackey, M.C. and Glass, L., Oscillation and chaos in physiological control systems, Science 197 (1977), 287
[9] Rey, A.D. and Mackey, M.C., Multistability and bounded layer development in a transport equation with delayed arguments, Can. App. Math. Quar. 1 (1993), 1
[10] Rey, A.D. and Mackey, M.C., Bifurcations and traveling waves in a delayed partial differential equation, CHAOS 2 (1992), 231